From ultra-filtration to fields irrigation: the reign of porous ducts

Antonio Fasano, Angiolo Farina
Dipartimento di Matematica "Ulisse Dini",
Università degli Studi di Firenze,
Viale Morgagni 67/A, I-50134 Firenze, Italy

Abstract

We review a large modeling work referring to flows through pipes having porous walls. Such a class of problems has important applications. Here we refer specifically to: ultrafiltration modules for water purification, irrigation techniques by means of porous (or dripping) pipes, and dialyzers. Despite the large differences among these devices, there are some common feature: in all cases the porous element has a cylindrical shape, with a radius which is much smaller than the length. This allows the use of an upscaling technique, starting from the basic equations at the microscale and leading to approximate macroscopic equations.

1 Introduction

Ultra-filtration is a technique employing porous membranes whose pores are in the submicron range (so to block large molecules). A typical device used in ultra-filtration processes is the hollow fibre, in which the porous membrane has a tubular shape. Such an element can be used in various flow configurations. The liquid to be filtered can cross the membrane from inside to outside (in-out flow) or vice versa (out-in flow). In addition, the terminal section of the element can be sealed (dead end mode), thus forcing the whole incoming liquid to cross the membrane, or the fluid can be allowed to flow out freely (cross flow mode). Clearly, the filtering action is more efficient in the dead end mode, which is frequently applied in water filtration plants, but it cannot be used for instance in dialyzers, where obviously blood has to be returned to the patients with all the cells it contains. Dialyzers are indeed another remarkable example of ultra-filtering devices employing hollow fibres, designed to perform operations normally carried out by kidneys. Though the dialyzer problem is by far more complicated, it shares with the water ultra-filtration modules many features that provide, so to speak, a common mathematical basis. The same can be said for another class of problems, namely the design of porous irrigation pipes, which possess several practical advantages (for instance reducing water evaporation, eliminating soil erosion, etc.). The related technology is not as sophisticated as for the previous devices, but it is interesting to notice that applying the same mathematical procedures leads to practical conclusions about the designing of such irrigation plants, depending on their size.

Thus, common mathematical ground is a good motivation for grouping together the three problems we want to deal with in this paper:

- modeling water ultra-filtration modules,
- modeling dialyzers,
- modeling porous irrigation pipes.

Of course we will confine to summarizing some results, since each of these subjects is quite large. The basic reference papers are respectively [3], [6], [7].

A peculiar aspect of dialyzers is that, since such devices continuously modify the blood composition, the input data have to keep track of the process history, thus exhibiting a memory effect. In addition we will see that boundary conditions are nonlocal in space too.

A more ambitious project is addressed to the mathematical modeling of kidneys. In that case the hollow fibre is nothing but the capillary vessel which winds up in the basic element of the kidney, namely the nephron. We plan to work on that problem in the next future. What we can say at this moment is that there are many important differences between the kidney (which performs many more functions) and the dialyzer, since their fluid dynamical regimes are basically different.

The novelty of the paper [3] in the framework of hollow fibres filters was the use of the upscaling procedure. This is a very general and well known method, exploiting the existence of a small parameter ε (namely the ratio between the fibres radius and their length) which goes through the following steps:

- write the Navier-Stokes equations for the ingoing and outgoing flows with the required initial and boundary conditions (for the flow across the membrane Darcy's law can be used directly),
- expand all quantities in power series of ε,
- match the terms with equal powers of ε in the above differential system.

Thus at each order of ε a differential system is obtained. Performing an average over the fibres cross section we are led to the equations governing the macroscopic (i.e. measurable) quantities. Hence the problem can be solved at the large scale at the desired approximation order. The basic advantage of the method consists in the fact that it is rooted in the physical principles, rather than using some heuristic basis to write directly some equations for the macroscopic variables.

Indeed, in [3] not only we got at the zero-order approximation the formulas already known, but we could write the first order corrections, investigating the influence of physical parameters (such as the one related to slip at the membrane interface, or the Reynolds number). It is useful to point out immediately that while slip at the membrane interface may be optional for ultra-filtration (and negligible for irrigation pipes), it is certainly very important for the case of the dialyzers.

Figure 1: *On the left: an example of hollow-fiber module. On the right: a magnified picture of a single hollow-fiber. Courtesy of Polymem - Toulouse, France.*

Thanks to the upscaling technique it was possible to obtain a rather detailed description of the dynamics of all the devices considered and the results are of practical interest.

2 Water ultrafiltration modules

The Life + European Contract *PURIFAST*, coordinated by New Technology Tecnotessile, Prato, Italy, of which the Math. Department U. Dini of the University of Florence is one of the partners, gave a great impulse to the study of the process of water ultra-filtration (both for industrial scope and for drinking water production). In the same direction acted the Contract *GOFIM*[1] coordinated by our Department (a rare event for an engineering project). The basic element of an ultra-filtration module is a hollow fibre, i.e. a tubular porous membrane. Thousands of such elements are encased in a module. There are various different arrangements and various different flow configurations. In the paper [3] we have studied the module represented in Fig. 1. The configuration was the one of dead-end, in-out flow, meaning that water is injected in the inner channel of the fibre, whose opposite end is sealed, so to force all the water to cross the membrane and flow back in the space among the fibres. The whole flow is driven by the transmembrane pressure, the difference between the pressure applied at the inlet surface and the pressure at which the so-called permeate is extracted.

The out-in flow configuration is also employed and can be studied in a very similar way

We must say that the study performed in [3] is confined to the dynamics of water through the device (with no impurities), which is already rather complicated. In the real industrial process impurities keep accumulating over the porous

[1] Financed by the Foundation for Research and Innovation of the University of Florence, Italy.

membrane forming a growing porous layer, whose effect is to reduce the flow because of the added hydraulic resistance and to the reduced lumen of the fibre. This phenomenon, called fouling, makes it necessary a repeated cleansing of the device which is carried out by means of a backwash cycle, periodically inverting the transbembrane pressure. In addition to the reversible fouling there is also a slower but progressive irreversible obstruction of the membrane pores, which eventually requires a chemical treatment and which limits the device lifetime. In the framework of *PURIFAST* all these phenomena have been modelled in the traditional way of introducing heuristic laws for the macroscopic quantities (see e.g. [2]). They can be dealt with by means of upscaling too, but since the required amount of work is not small, we have postponed this project.

Let us now summarize the results of [3].

2.1 Reduction to a single fibre

The first simplification consists in isolating one fibre in the bundle making the ultra-filtration module. This is made possible by symmetry reasons, since, with the exception of the relatively few fibres in the peripheral zone of the module, we may say that each fibre is surrounded by a cylinder of hexagonal cross section which is actually a no flow surface. It has been proved in [3] that for the geometry of a filter (and of a dialyzer) the isolating cylinder can be taken to have a circular cross section (the relative error being very small). Thus from now on we consider the flow domains illustrated in Fig. 2.

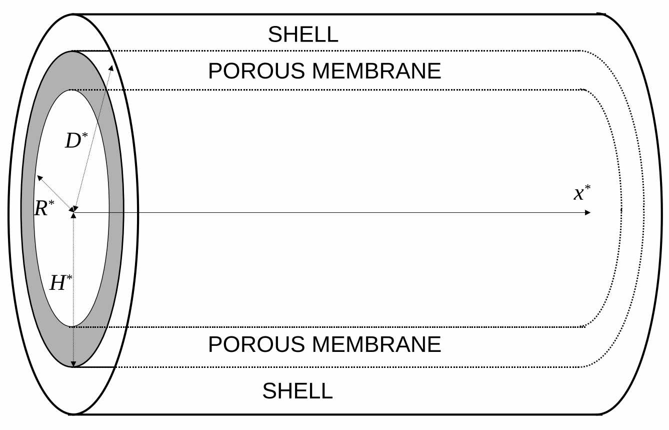

Figure 2: *A schematic representation of the cylindrical domains.*

Henceforth we will deal with the flow in the cylindrical domain composed by[2]:

- The inner channel[3] $0 < r^* < R^*$ (velocity field $\vec{v}^*$).
- The porous wall or membrane $R^* < r^* < H^*$ (velocity field $\vec{u}^*$).
- The permeate flow domain or shell $H^* < r^* < D^*$ (velocity field $\vec{w}^*$). We remark that D^* is the equivalent radius of the external cylinder, which can be expressed explicitly in terms of the fibre external radius H^* and of the distance E^* between the axes of contiguous fibres in the array: $2\pi D^{*\,2} = \sqrt{3}E^{*\,2}$.

The thickness of the fiber is

$$S^* = H^* - R^*.$$

In practical cases

$$\frac{H^* - R^*}{R^*} = \mathcal{O}\left(1\right), \quad \text{and} \quad \frac{D^* - H^*}{H^*} = \mathcal{O}\left(1\right),$$

typical orders of magnitude are: $R^* \sim 100\ \mu m$, and $S^* \sim 50\ \mu m$.

The fiber length is L^*. A key assumption of our study is that

$$\varepsilon = \frac{R^*}{L^*} \ll 1.$$

Usually $L^* \sim 1\,m$, so that $\varepsilon \sim 10^{-4}$. To be specific, we refer the readers to the data reported in [4], [5] and [11].

We consider the Navier Stokes equation for the incompressible flow in the inner channel and in the outer shell, supposing that in both cases we have a laminar regime (by assumption the liquid is the same), and we describe the flow through the membrane by means of Darcy's law.

The boundary conditions are:

- Inlet pressure $p^*_{in}\left(t^*\right)$, at $x^* = 0,\ 0 < r^* < R^*$.
- Outlet pressure $p^*_{out}\left(t^*\right) < p^*_{in}\left(t^*\right)$, at $x^* = 0,\ H^* < r^* < D^*$.
- No flux at $x^* = L^*$.
- No flux at $r^* = D^*$.
- Slip conditions at both interfaces $r^* = R^*,\ r^* = H^*$.

[2] Throughout this paper the superscript "$*$" denotes dimensional variables.

[3] x^* denotes the longitudinal coordinate, while r^* the radial one. Due to rotational symmetry, the azimuthal coordinate never appears.

The slip conditions (according to Beavers and Joseph [1]) involve the jump of the longitudinal component of the fluid velocity across interfaces separating a Navier-Stokes flow and a Darcy flow: the jump is proportional to the normal derivative of the considered component, evaluated on the side of the Navier-Stokes regime. Since the longitudinal velocity within the membrane is very small, the Beavers-Joseph condition is practically equivalent to the Saffman condition [14], in which such a component is neglected. We will write the slip boundary conditions directly in the dimensionless form in the next section.

2.2 The double scaling and the dimensionless system

The key geometrical feature ensuring $\varepsilon \ll 1$, suggest to use two different scales for the coordinates x^*, r^*, as well as for the longitudinal and the radial components of the three velocity fields. We use the dimensionless coordinates

$$x = \frac{x^*}{L^*}, \quad r = \frac{r^*}{R^*}.$$

We also introduce $H = H^*/R^*$, and $S = S^*/R^*$, and the two characteristic velocities v_c^*, u_c^*, $u_c^* = \varepsilon v_c^*$, for Navier-Stokes and for Darcian flows, respectively. Next we define a characteristic time $t_c^* = L^*/v_c^*$, which we select as reference time scale, so that $t = t^*/t_c^*$, is the dimensionless time variable.

The rescaled velocity components are defined as follows

$$v_x = \frac{v_x^*}{v_c^*}, \quad v_r = \frac{v_r^*}{\varepsilon\, v_c^*}, \quad u_x = S\varepsilon \frac{u_x^*}{u_c^*}, \quad u_r = \frac{u_r^*}{u_c^*}, \quad w_x = \frac{w_x^*}{w_c^*}, \quad w_r = \frac{w_r^*}{\varepsilon\, w_c^*}.$$

The natural way of defining v_c^* is to refer to the total inlet discharge $\dot{V}_{in}^*$, writing $\dot{V}_{in}^* = 2\pi R^* v_c^*$ (then the definition of u_c^* is consistent with the equality of the incoming and of the outgoing liquid volume rate). For the fibres of ultrafiltration modules typical values are $v_c^* \sim 10\ cm/s$.

The inner channel pressure is rescaled by

$$p_{h,\,c}^* = \frac{v_c^* \mu^* L^*}{R^{*2}},$$

obtained considering a laminar flow of Newtonian fluid, whose viscosity is μ^*, in a tube of radius R^* with the mean velocity v_c^*.

Concerning the membrane, we denote by $p_{m,\,c}^*$ the fluid characteristic pressure. We define it in the spirit of Darcy's law, i.e.

$$p_{m,\,c}^* = \frac{n\mu^*}{K^*}\, S^* u_c^*,$$

where n is the membrane porosity and K^* the membrane permeability (uniform and isotropic). Note that

$$\frac{p_{m,\,c}^*}{p_{h,\,c}^*} = \varepsilon^2\, \gamma, \quad \text{with} \quad \gamma = \frac{n R^{*\,2}}{K^*}.$$

The parameter $\Gamma = \varepsilon^2 \gamma = \dfrac{n\, R^{*\,4}}{L^{*\,2} K^{*}}$, has also a basic role, as well as ε, Re. We will just consider $\Gamma = \mathcal{O}(1)$, since for the filtration modules $\Gamma \sim 0.1$.

Let us now write the whole system of dimensionless equations.

(I) **The inner fibre channel** $(0 < x < 1,\ 0 < r < 1)$.

The non–dimensional version of the continuity equation is

$$\frac{\partial v_x}{\partial x} + \frac{1}{r}\frac{\partial}{\partial r}(r\, v_r) = 0, \tag{2.1}$$

and the dimensionless form of the Navier–Stokes equations is

$$\frac{\mathsf{Re}}{\varepsilon}\left[\frac{\partial v_x}{\partial t} + v_x \frac{\partial v_x}{\partial x} + v_r \frac{\partial v_x}{\partial r}\right] = -\frac{1}{\varepsilon^2}\frac{\partial p_h}{\partial x} + \frac{\partial^2 v_x}{\partial x^2} + \frac{1}{\varepsilon^2}\frac{1}{r}\frac{\partial}{\partial r}\left(r \frac{\partial v_x}{\partial r}\right), \tag{2.2}$$

$$\begin{aligned}\frac{\mathsf{Re}}{\varepsilon}\left[\frac{\partial v_r}{\partial t} + v_x \frac{\partial v_r}{\partial x} + v_r \frac{\partial v_r}{\partial r}\right] &= -\frac{1}{\varepsilon^4}\frac{\partial p_h}{\partial r} + \frac{\partial^2 v_r}{\partial x^2} \\ &\quad + \frac{1}{\varepsilon^2}\left(\frac{1}{r}\frac{\partial}{\partial r}\left(r\frac{\partial v_r}{\partial r}\right) - \frac{v_r}{r^2}\right),\end{aligned} \tag{2.3}$$

where p_h is the dimensionless pressure within the channel and where

$$\mathsf{Re} = \frac{\rho^*\, v_c^* R^*}{\mu^*} = \frac{\rho^* R^{*\,2}}{\mu^{*\,2}} \frac{\varepsilon}{S\,\Gamma} p^*_{m,\,c}\,, \tag{2.4}$$

is the the Reynolds number. In particular, we suppose $\mathsf{Re} \le \mathcal{O}(1)$, i.e. implies laminar flow.

The inlet boundary condition is $p_h(0, r, t) = p_{in}(t)$, the dead-end condition $v_x(1, r, t) = 0$, and the symmetry condition on the axis $v_r(x, 0, t) = 0$, $\frac{\partial v_x(0,x,t)}{\partial x} = 0$.

(II) **The flow in the membrane** $(0 < x < 1,\ 1 < r < H)$.

Darcy's law

$$\begin{cases} u_x = -S^2 \varepsilon^2 \dfrac{\partial p_m}{\partial x}, \\[2ex] u_r = -S \dfrac{\partial p_m}{\partial r}, \end{cases}$$

which, when combined with the continuity equation, gives the following equation for the pressure p_m

$$\frac{\partial^2 p_m}{\partial x^2} + \frac{1}{\varepsilon^2}\frac{1}{r}\frac{\partial}{\partial r}\left(r \frac{\partial p_m}{\partial r}\right) = 0. \tag{2.5}$$

(III) **The permeate flow** $(0 < x < 1,\ H < r < D)$.

With the same definition of Re as in (I) we have[4]

$$\begin{aligned}\frac{\mathsf{Re}}{\varepsilon}\left[\frac{\partial w_x}{\partial t}+w_x\frac{\partial w_x}{\partial x}+w_r\frac{\partial w_x}{\partial r}\right] &= -\frac{1}{\varepsilon^2}\frac{\partial p_v}{\partial x}+\frac{\partial^2 w_x}{\partial x^2}\\ &+\frac{1}{\varepsilon^2}\frac{1}{r}\frac{\partial}{\partial r}\left(r\frac{\partial w_x}{\partial r}\right),\end{aligned} \tag{2.6}$$

$$\begin{aligned}\frac{\mathsf{Re}}{\varepsilon}\left[\frac{\partial w_r}{\partial t}+w_x\frac{\partial w_r}{\partial x}+w_r\frac{\partial w_r}{\partial r}\right] &= -\frac{1}{\varepsilon^4}\frac{\partial p_v}{\partial r}+\frac{\partial^2 w_r}{\partial x^2}\\ &+\frac{1}{\varepsilon^2}\left(\frac{1}{r}\frac{\partial}{\partial r}\left(r\frac{\partial w_r}{\partial r}\right)-\frac{w_r}{r^2}\right),\end{aligned} \tag{2.7}$$

and the continuity equation

$$\frac{\partial w_x}{\partial x}+\frac{1}{r}\frac{\partial}{\partial r}\left(r\,w_r\right)=0. \tag{2.8}$$

To (2.6)–(2.8), we associate the boundary conditions at $r = D$ (no cross flow and symmetry of the longitudinal flow) $\left.\frac{\partial w_x}{\partial r}\right|_{r=D}=0$, $\left.w_r\right|_{r=D}=0$, $x = 1$ (dead-end) $\left.w_x\right|_{x=1}=0$, and at the outlet surface $x = 0$, $\left.p_v\right|_{x=0}=p_{in}(t)-\Delta p(t)$.

(IV) **Conditions at the interfaces** $(0 < x < 1,\ r = 1$ and $r = H\ )$.

Continuity of pressure is expressed as

$$\left.p_h\right|_{r=1}=\Gamma\ \left.p_m\right|_{r=1}\ , \quad \left.p_v\right|_{r=H}=\Gamma\ \left.p_m\right|_{r=H}\ , \tag{2.9}$$

where the presence of Γ is due to the different rescaling of the two pressures.

The flux continuity (mass conservation) takes the form

$$v_r\left(x,1,t\right)=-n\left.\frac{\partial p_m}{\partial r}\right|_{r=1}, \qquad \left.w_r\right|_{r=H}=-n\left.\frac{\partial p_m}{\partial r}\right|_{r=H}.$$

Now we write down the slip conditions as follows

$$\left.v_x\right|_{r=1}=-\frac{1}{\mathsf{B}}\left.\frac{\partial v_x}{\partial r}\right|_{r=1}, \qquad \left.w_x\right|_{r=H}=\frac{1}{\mathsf{B}}\left.\frac{\partial w_x}{\partial r}\right|_{r=H}, \tag{2.10}$$

which are the so called Saffman's conditions. In [10] the practical equivalence of Saffman's to Beaver-Joseph conditions has been proved (and in our case the two conditions differ for an $\mathcal{O}\left(\varepsilon^2\right)$ term).

From (2.10) it looks evident that the situation in which slip is influential at the order zero in ε is that $\mathsf{B}=\mathcal{O}(1)$ or less, while $\mathsf{B}=\mathcal{O}\left(\varepsilon^{-m}\right)$ will affect the m^{th} order correction (m positive integer).

[4] p_v denotes the dimensionless pressure in the shell.

How to prescribe B is not trivial. Somebody claims that for low porosity media it is proportional to $n^{-1/2}$ (see [15]). For the ultrafiltration modules it turns out that slip is not important at the zero order approximation, but there is a strong experimental evidence that slip is of paramount importance in dialyzers (as it is in blood vessels). Therefore we keep B in the formulae which follow, remarking that if we measure the transmembrane pressure and the discharge our model provides a way of deducing the characteristic slip parameter B.

2.3 Upscaling

We now consider the equations (2.1)–(2.2), (2.5)–(2.8) , expanding each unknown in powers of ε and matching the coefficients in the resulting series. We keep the procedure at a formal level, i.e. we do not consider the question of convergence.

At the zero order approximation we find that pressures $p_h^{(0)}$, $p_v^{(0)}$, are independent of r (meaning that they are already macroscopic quantities), and we get the following differential system

$$\begin{cases} -\dfrac{\partial p_h^{(0)}}{\partial x} + \dfrac{1}{r}\dfrac{\partial}{\partial r}\left(r\dfrac{\partial v_x^{(0)}}{\partial r}\right) = 0, \\[2ex] \dfrac{\partial}{\partial r}\left(r\, v_r^{(0)}\right) = -r\dfrac{\partial v_x^{(0)}}{\partial x} = \dfrac{\partial^2 p_h^{(0)}}{\partial x^2}\left[\dfrac{r}{2\mathsf{B}} + \dfrac{r}{4}\left(1-r^2\right)\right], \\[2ex] \dfrac{\partial}{\partial r}\left(r\dfrac{\partial p_m^{(0)}}{\partial r}\right) = 0, \\[2ex] \dfrac{1}{r}\dfrac{\partial}{\partial r}\left(r\dfrac{\partial w_x^{(0)}}{\partial r}\right) = \dfrac{\partial p_v^{(0)}}{\partial x}, \\[2ex] \dfrac{\partial}{\partial r}\left(r\, w_r^{(0)}\right) = r\psi\left(r\right)\dfrac{\partial^2 p_v^{(0)}}{\partial x^2}, \end{cases}$$

where

$$\psi\left(r\right) = \frac{1}{2}\left\{\frac{D^2-H^2}{\mathsf{B}\,H} + \left[D^2\ln\left(\frac{r}{H}\right) - \frac{1}{2}\left(r^2-H^2\right)\right]\right\}.$$

The first two equations describe the flow in the inner channel, the third equation relates to the flow across the membrane, and the last pair of equations governs the permeate flow.

Using the boundary conditions we can perform some integrations and we obtain

$$p_m^{(0)}\left(x,r,t\right) = p_h^{(0)}\left(x,t\right) + \frac{p_v^{(0)}\left(x,t\right) - p_h^{(0)}\left(x,t\right)}{\ln H}\ln r,$$

and

$$w_x^{(0)}(x,r,t) = w_x^{(0)}(x,H,t) - \frac{1}{2}\frac{\partial p_v^{(0)}(x,t)}{\partial x}\left[D^2 \ln\left(\frac{r}{H}\right) - \frac{1}{2}\left(r^2 - H^2\right)\right],$$

with

$$w_x^{(0)}(x,H,t) = -\frac{D^2 - H^2}{2\mathsf{B}\,H}\frac{\partial p_v^{(0)}}{\partial x},$$

whence

$$\begin{aligned} w_x^{(0)}(x,r,t) &= -\psi(r)\,\frac{\partial p_v^{(0)}}{\partial x}, \\ w_r^{(0)}(x,r,t) &= -\Psi(r)\,\frac{\partial^2 p_v^{(0)}}{\partial x^2}, \end{aligned}$$

with

$$\begin{aligned} \Psi(r) &= \frac{1}{r}\int_r^D r'\,\psi(r')\,dr' \\ &= \frac{1}{2r}\left[\left(D^2 - H^2\right)\left(\frac{1}{2\mathsf{B}H} - \frac{1}{4}\right) - \frac{1}{8}\left(D^2 + r^2\right)\right]\left(D^2 - r^2\right) \\ &\quad + \frac{D^2}{2r}\left[\ln\left(\frac{D}{H}\right)\frac{D^2}{2} - \ln\left(\frac{r}{H}\right)\frac{r^2}{2}\right]. \end{aligned} \tag{2.11}$$

Of course, $\Psi(r) > 0$ for $r \in [H,D]$, since, as remarked, ψ is positive for $H \le r \le D$.

We thus, recalling the interface conditions, we get to

$$\frac{\partial^2 p_v^{(0)}}{\partial x^2} = A\left[p_v^{(0)}(x,t) - p_h^{(0)}(x,t)\right], \tag{2.12}$$

$$\frac{\partial^2 p_h^{(0)}}{\partial x^2} = -C\left[p_v^{(0)}(x,t) - p_h^{(0)}(x,t)\right], \tag{2.13}$$

where

$$\begin{aligned} A &= \frac{n}{\Gamma\,H\,\Psi(H)\ln H} = \frac{1}{H\,\Psi(H)}\frac{K^* L^{*\,2}}{R^{*\,4}\ln\left(\dfrac{H^*}{R^*}\right)} \\ &= \frac{16}{H^4}\left\{\left[4\left(\frac{D}{H}\right)^4\ln\left(\frac{D}{H}\right) + 4\left(\frac{D}{H}\right)^2 - 3\left(\frac{D}{H}\right)^4 - 1\right]\right. \\ &\quad \left. + \frac{4}{\mathsf{B}H}\left(\left(\frac{D}{H}\right)^2 - 1\right)^2\right\}^{-1}\frac{K^* L^{*\,2}}{R^{*\,4}\ln\left(\dfrac{H^*}{R^*}\right)}, \end{aligned}$$

and

$$C=\frac{4n}{\Gamma\left(\frac{1}{\mathsf{B}}+\frac{1}{4}\right)\ln H}=\frac{256}{\left(\frac{4}{\mathsf{B}}+1\right)}\frac{K^{*}\,L^{*\,2}}{\left(2R^{*}\right)^{4}\ln\left(\frac{H^{*}}{R^{*}}\right)}.$$

Of course, (2.12), (2.13) have to be supplemented with the boundary conditions

$$p_h^{(0)}\left(0,t\right)=p_{in}\left(t\right),\qquad p_v^{(0)}\left(0,t\right)=p_{in}\left(t\right)-\Delta p\left(t\right),\qquad \left.\frac{\partial p_h}{\partial x}\right|_{x=1}=\left.\frac{\partial p_v}{\partial x}\right|_{x=1}=0.$$

Introducing the difference

$$\Pi\left(x,t\right)=p_v^{(0)}\left(x,t\right)-p_h^{(0)}\left(x,t\right),$$

we find that it satisfies the boundary value problem

$$\begin{cases}\dfrac{\partial^2\Pi}{\partial x^2}=\left(A+C\right)\Pi,\\[2ex] \left.\dfrac{\partial\Pi}{\partial x}\right|_{x=1}=0,\\[2ex] \Pi\left(0,t\right)=\Delta p\left(t\right),\end{cases}$$

for which we have the explicit solution

$$\Pi=-\frac{\Delta p\left(t\right)}{1+e^{-2\sqrt{A+C}}}\left(e^{-\sqrt{A+C}\,x}+e^{\sqrt{A+C}\left(x-2\right)}\right).$$

We can now go back to the problem of finding the pressure profile in the incoming and outgoing fluxes, which can be expressed in terms of Π

$$\begin{aligned}p_v^{(0)}\left(x,t\right)&=\left(p_{in}\left(t\right)-\Delta p\left(t\right)\right)-A\int_0^x\left(\int_{x'}^1\Pi\left(x'',t\right)\,dx''\right)dx',\\ p_h^{(0)}\left(x,t\right)&=p_{in}\left(t\right)+C\int_0^x\left(\int_{x'}^1\Pi\left(x'',t\right)\,dx''\right)dx',\end{aligned}$$

and the corresponding longitudinal velocity fields

$$\begin{aligned}v_x^{(0)}\left(x,r,t\right)&=\left[\frac{1}{2\mathsf{B}}+\frac{1}{4}\left(1-r^2\right)\right]\frac{C\,\Delta p\left(t\right)}{1+e^{-2\sqrt{A+C}}}\int_x^1\left(e^{-\sqrt{A+C}\,x'}\right.\\ &\qquad\left.+e^{\sqrt{A+C}\left(x'-2\right)}\right)dx',\\ w_x^{(0)}\left(x,r,t\right)&=-\psi\left(r\right)\frac{A\,\Delta p\left(t\right)}{1+e^{-2\sqrt{A+C}}}\int_x^1\left(e^{-\sqrt{A+C}\,x'}+e^{\sqrt{A+C}\left(x'-2\right)}\right)dx'.\end{aligned}$$

Thus we have emphasized in particular the dependence on the slip coefficient B.

The formulae above provide the expression of the total volumetric discharge of a single fibre in the array

$$\dot{V}^{(0)} = 2\pi \int_0^1 v_x^{(0)}(0, r, t)\, r dr = 2\pi \frac{\varphi\, \Delta p\,(t)}{\sqrt{A+C}\, \ln H} \frac{1 - e^{-2\sqrt{A+C}}}{1 + e^{-2\sqrt{A+C}}}.$$

Using dimensional variables, the formula for the discharge has the structure

$$\dot{V}^{*(0)} = 2\pi \frac{K^* L^{*\,2}}{\mu^*} \mathcal{K}_{eff} \frac{\Delta p^*}{L^*},$$

with the expected proportionality to the ratio between the transmembrane pressure and the fibre length through the hydraulic conductivity of the membrane, with the coefficient

$$\mathcal{K}_{eff} = \frac{1}{\sqrt{A+C}\ln H} \frac{1 - e^{-2\sqrt{A+C}}}{1 + e^{-2\sqrt{A+C}}}$$

providing the correction due to the geometry and the regime chosen for the flow.

It is also possible to proceed to calculating the first order corrections. We omit such a further step because expressions become very large, but we report one significant result: at the first order the relationship between discharge and transmembrane pressure ceases to be linear. A quadratic term appears which turns out to be proportional to Reynolds' number. Thus for Re not too small such a correction may be important.

In conclusion we can say that the upscaling procedure is rather versatile and very effective. Not only it provides rigorous expressions for the relevant macroscopic quantities at the zero order, which agree with the ones basically already known to the engineers, but it provides the corrections due to the geometry (surprisingly the formulae available in the engineering literature [16], [5] do not contain the factor $\ln H$ coming from the cylindrical shape), but it also allows to evaluate the influence of slip and the deviations from linearity, detectable at higher order approximations.

3 Irrigation pipes

Since ancient times it was known that a very convenient way of delivering water to plants in dry regions was to bury clay pots full of water close to the roots. That method has the obvious advantage of not wasting excess water and above all of reducing evaporation. In modern times the evolution of this technique was the construction of irrigation plants consisting of pipes laid down or suspended on the ground and leaking water either because there are made with a porous material, or because the wall are suitably treated for that purpose (for instance drilling dripping holes). The flow mode is, here too, characterized by the dead-end configuration.

The first reported study on a large scale plant is [13]. In the paper [7] the upscaling technique was applied to analyze two classes of models: one for small

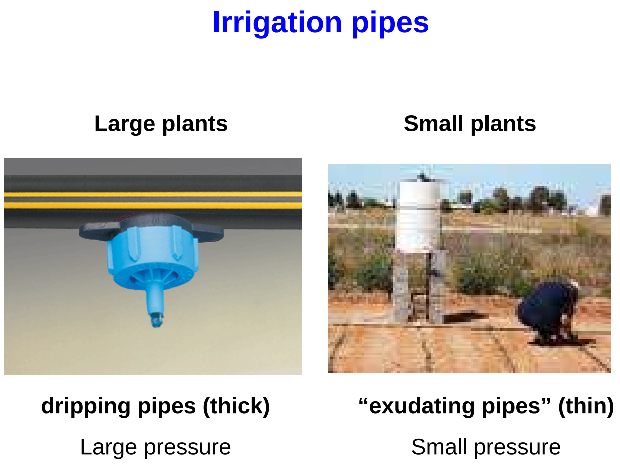

Figure 3: *On the left: an example of hollow pipe used in large plants. On the right: a small plant.*

scale and one for large scale plants. In small scale plants we have a typical length of 100 m and pipes are made of canvas (typical thickness: 1 mm). The pipe is connected to a small reservoir (see Fig. 3) (typical capacity $\sim 1\ m^3$), placed at some elevation (1 m) to provide the driving pressure (typical order $\sim 10\ Kpa$), which has to be refilled periodically. In large plants the required pressure is much larger and therefore the pipes are usually made with an impermeable material with dripping sites periodically distributed. The problem may look simple (particularly for the kitchen garden scale), but it turns out to be absolutely not trivial. For instance a not intuitive question is how to select both the geometry and the material so to have a sufficiently uniform water delivery rate along the pipe.

Modeling proceeds differently for the small and for the large scale plants. Here we confine to the former case.

We take the following reference quantities: pipe length $L^* = 100\ m$, pipe internal radius $R^* = 5\ mm$, wall thickness $S^* = 1\ mm$. We leave the permeability as a quantity to be chosen so to satisfy the criterion of an efficient water supply to the ground. According to the data above $\varepsilon \sim 5 \cdot 10^{-5}$, so very similar to the previous case. What changes here in the geometry is the fact that the ratio S^*/R^* is smaller than the one of hollow fibres. The most substantial change is that the average water velocity is much smaller.

The differential equations for the main flow and for the cross flow through the pipe are the same as in the case of the hollow fibres. Some of boundary conditions are instead different. Let us just write the system of boundary conditions, using the same symbols as in the previous section

$$\begin{aligned}
p_h^*(0,r^*,t^*) &= P_{in}^*(t^*), \quad \text{(prescribed inlet pressure)}, && (3.14)\\
p_m^*(x^*,H^*,t^*) &= 0, \quad \text{(atmospheric pressure)}, && (3.15)\\
p_h^*(R^*,r^*,t^*) &= p_m^*(R^*,r^*,t^*), \quad \text{(pressure continuity)}, && (3.16)\\
v_r^*(x^*,R^*,t^*) &= n\, u_r^*(x^*,R^*,t^*), \quad \text{(flux continuity)}, && (3.17)\\
v_x^*(x^*,R^*,t^*) &= 0, \quad (\text{no} - \text{slip}), && (3.18)\\
v_x^*(L^*,r^*,t^*) &= 0, \quad (\text{dead} - \text{end}), && (3.19)\\
v_r^*(x^*,0,t^*) &= 0, \quad \text{(symmetry)}, && (3.20)\\
\left.\frac{\partial v_x^*}{\partial r^*}\right|_{r^*=0} &= 0, \quad \text{(symmetry)}. && (3.21)
\end{aligned}$$

Condition (3.14) specifies the inlet pressure: in gravity fed pipes the time dependence is due to the progressive draining of the reservoir. It is important to remark that in this case the function $P_{in}^*(t)$ is unknown.

Now we proceed to the double rescaling of the space and time coordinate, and of the components of the two velocity fields, basically in the same way we did for the hollow fibre (see section 2.2). However we take a different definition of the characteristic longitudinal velocity v_c^*, by first selecting a typical discharge q_c^* and then posing

$$q_c^* = \pi R^{*\,2} v_c^*.$$

Indeed, in the present case it makes sense to impose the draining time of the reservoir, thus q_c^*.

Accordingly the new characteristic time will be $t_c^* = \pi R^{*\,2} L^*/q_c^*$, namely the ratio between the volume of the water filling the pipe and the characteristic discharge.

For rescaling pressure in the pipe we refer to a standard Poiseuille flow with an average velocity $v_c^*/2$ (to take into account the dead end condition) and we select

$$p_c^* = \frac{4 v_c^* \mu^* L^*}{R^{*\,2}}.$$

It is convenient to rescale both p_h^* and p_m^* by p_c^* (so the continuity condition at interface is simply written as equality of the dimensionless pressures). Nevertheless it is also useful to define a reference pressure for the cross flow, namely $p_{m\ c}^* = \varepsilon v_c^* \mu^* S^*/2K^*$, in such a way that the pressure gradient $p_{m\ c}^*/S^*$, produces the Darcy velocity εv_c^*. Indeed, if we want that the ratio[5]

$$\chi = \frac{p_{m\ c}^*}{p_c^*} = \frac{\varepsilon^2}{8}\frac{S}{\mathsf{Da}}, \tag{3.22}$$

[5] $\mathsf{Da} = K^*/R^{*\,2}$, Darcy number.

is $\mathcal{O}(1)$, then we need the Darcy number $\mathsf{Da} \sim 6 \cdot 10^{-11}$, meaning $K^* \sim 10^{-15}\, m^2$. In this way we have readily established the expected order of magnitude of the pipe wall permeability.

The entire dimensionless system has the form

$$
\begin{aligned}
&\frac{\partial v_x}{\partial x} + \frac{1}{r}\frac{\partial}{\partial r}(r\, v_r) = 0,\\
&\frac{\mathsf{Re}}{\varepsilon}\left[\frac{\partial v_x}{\partial t} + v_x\frac{\partial v_x}{\partial x} + v_r\frac{\partial v_x}{\partial r}\right] = -\frac{1}{\varepsilon^2}\frac{\partial p_h}{\partial x} + \frac{\partial^2 v_x}{\partial x^2} + \frac{1}{\varepsilon^2}\frac{1}{r}\frac{\partial}{\partial r}\left(r\frac{\partial v_x}{\partial r}\right),\\
&\frac{\mathsf{Re}}{\varepsilon}\left[\frac{\partial v_r}{\partial t} + v_x\frac{\partial v_r}{\partial x} + v_r\frac{\partial v_r}{\partial r}\right] = -\frac{1}{\varepsilon^4}\frac{\partial p_h}{\partial r} + \frac{\partial^2 v_r}{\partial x^2}\\
&\qquad\qquad\qquad\qquad\qquad\qquad + \frac{1}{\varepsilon^2}\left(\frac{1}{r}\frac{\partial}{\partial r}\left(r\frac{\partial v_r}{\partial r}\right) - \frac{v_r}{r^2}\right),\\
&\frac{\partial u_x}{\partial x} + \frac{1}{r}\frac{\partial}{\partial r}(r\, u_r) = 0,\\
&u_r = -\frac{S}{\chi}\frac{\partial p_m}{\partial x},\\
&u_x = -\varepsilon^2\frac{S}{\chi}\frac{\partial p_m}{\partial x},\\
&p_h|_{x=0} = P_{in}(t) = \frac{P^*_{in}(t)}{p^*_c}, \quad p_h|_{r=1} = p_m|_{r=1}, \quad p_m|_{r=H} = 0,\\
&v_r|_{r=1} = u_r|_{r=1}, \quad v_x|_{r=1} = 0, \quad v_x|_{x=1} = 0,\\
&v_r|_{r=0} = 0, \quad \left.\frac{\partial v_x}{\partial r}\right|_{r=0} = 0,
\end{aligned}
$$

where Re is the Reynolds number. As for the case of hollow fibres, we would like to neglect the inertia terms. However, since R^* is much larger in this case, we cannot have $\mathsf{Re} \sim 1$. Also, we want the motion to be laminar, since we have used Navier-Stokes equations. A compromise is to take $\mathsf{Re} = 1000 \div 2000$, (considering that the actual reference velocity is $v^*_c/2$). In that way the inequality $\mathsf{Re} \ll 1/\varepsilon$, is still satisfied. To $\mathsf{Re} = 1500$ it corresponds $R^* v^*_c = 1.5 \cdot 10^{-3}\ m^2/s$, and a total discharge $q^*_c \sim 2.2\ m^3/day$. Usual values of range between 1 and 3 m^3/day. Therefore our approach is correct (for pipes of the given size).

We refer to [7] for the details of the upscaling procedure and for the formulation of the zero order approximation model, as well as for its integration. Here we report the main result, which concerns the dimensionless velocity of the main flow

$$
v_x^{(0)}(x,r,t) = P_{in}(t)\, C\left[\frac{e^{-Cx}}{1+e^{-2C}} + \frac{e^{Cx}}{1+e^{2C}}\right]\left(1-r^2\right), \tag{3.23}
$$

$$
v_r^{(0)}(x,r,t) = \frac{P_{in}(t)}{2} C^2\left[\frac{e^{-Cx}}{1+e^{-2C}} + \frac{e^{Cx}}{1+e^{2C}}\right] r\left(1-\frac{r^2}{2}\right), \tag{3.24}
$$

where $C^2 = \dfrac{4S}{\chi \ln(1+S)}$.

We also write the expression of the dimensionless cross velocity

$$u_r^{(0)}(x,r,t) = \frac{P_{in}(t)}{4r} C^2 \left[\frac{e^{-Cx}}{1+e^{-2C}} + \frac{e^{Cx}}{1+e^{2C}} \right], \tag{3.25}$$

which allows us to formulate the condition of "efficient watering" by imposing that the ratio

$$\Upsilon = \frac{u_r^{(0)}(1,1,t)}{u_r^{(0)}(0,1,t)} = \frac{1}{\cosh C}$$

is sufficiently close to 1. That amounts to prescribing the value of C

$$C = \ln \left[\frac{1}{\Upsilon} \left(1 + \sqrt{1-\Upsilon} \right) \right].$$

In turn this is equivalent to select the ratio χ, defined by (3.22), as

$$\chi = \frac{4S}{C^2 (1+S)}.$$

We thus deduce in turn the value of Da. For instance, if we take $\Upsilon = 0.8$, we finally obtain the wall permeability $K^* = 5 \cdot 10^{-15}\ m^2$, ensuring that at the end of the tube the water delivery rate is 80% of the one at the entrance. Another information we can retrieve is the initial elevation of the water free surface in the reservoir, corresponding to a selected total discharge. To $q_c^* = 2 \cdot 10^{-5}\ m^3/s \sim 1.73\ m^3/day$, it corresponds $P_{in}^* \sim 18\ KPa$, i.e. an elevation of $1.8\ m$. This result is interesting, but it does not solve the whole problem yet. Indeed we still have to find how the inlet pressure $P_{in}^*(t)$ evolves when the reservoir is progressively drained[6]. This last step is very easy. Let the reservoir be a cylinder of radius R_{res}^* and height H_{res}^* and let be h_o^* the elevation of its basis on the ground. Equation (3.24) (or (3.25)) gives the total discharge in the form

$$Q(t) = AP_{in}(t), \quad \text{where} \quad A = \frac{C}{2} \frac{\sinh(2C)}{1+\cosh(2C)}.$$

At the same time the dimensionless elevation h (height is rescaled by H_{res}^*) obeys the simple equation

$$\frac{dh}{dt} + AB(h + h_o) = 0,$$

where

$$B = \frac{\pi R^{*\ 4} \rho^* g^*}{4\mu^* q_c^*} \left(\frac{R^*}{R_{res}^*} \right).$$

Calculating $h(t)$ is now trivial.

[6]Such a pressure can be maintained at is initial value by providing water at the same rate at which it is delivered to the ground along the whole pipe (which can be calculated since in that case the pressure is known). Alternatively, one can think of a periodic automatic (or manual) refill of the reservoir. Here we just consider a situation in which no extra water is supplied.

4 Hemodialyzers

4.1 Targets and working conditions

In the paper [6] we have applied the upscaling technique to the analysis of a dialyzer using hollow fibres. Of course there are some similarities with the ultrafiltration module, but the problem is basically different for many reasons. First of all the flow mode of blood is different: the blood is taken from a patient's artery and returned to a patient's vein. Moreover, the nature of the fluid is peculiar: blood has to be treated as a mixture of plasma and of a cellular component (largely made of Red Blood Cells, RBC's). This has several consequences on the rheology. The composite nature of blood comes naturally into play, since RBC's do not cross the membrane and they do not adhere to the fibre wall, thus producing a slip of the mixture. In the space among the fibres there is a counter-flow, driven by an independent pressure gradient, having the task of removing the dialyzate. The latter is a fluid that is supplied at the counter-flow inlet with some composition (in balance with the concentration of substances that do not have to be removed from blood) and that leaves the device enriched by urea, creatinine, etc., i.e. of the noxious substances that have to be diluted in blood. An essential task that have to be performed by the dialyzer is the removal from blood of an important quantity of water, to compensate the decrease of hematocrit (RBC's volume fraction) due to renal dysfunction. To have an idea, the total volume of blood in a normal individual is around 5 liters. This value is largely altered by renal dysfunction in the course of a few days. In one dialysis treatment the volume of plasma to be extracted can be around 3 liters, thus increasing the hematocrit from the value prior to treatment ($\sim$ 0.3) to the normal value ($\sim$ 0.45). In summary, the treatment has to reach two targets:

(i) the desired value of hematocrit,

(ii) the desired level of noxious substances.

Such goals are not generally achieved at the same time, since the kind of device we are considering (the so-called fast dialyzer) is very effective in removing plasma. This high plasma extraction rate favors also the removal of urea etc., adding its action to diffusion. Therefore at a certain point the treated blood is enriched with plasma before being returned to the vein. For other details (addition of anticoagulants, etc.) see the technical papers [8], [9], [12].

During the treatment three operating conditions have to be satisfied:

(a) blood counterflow from the vein must be prevented,

(b) the outlet blood flux must be compatible with the one in the receiving vessel,

(c) shear stress exerted on RBC's must stay far from the threshold of hemolysis.

These conditions translate into constraints on the geometrical and physical parameters of the device.

4.2 The dimensionless model

The preliminary operation is to single out one fibre, surrounded by an ideal impervious cylindrical boundary, as we have done for the ultrafiltration module.

For lack of space we confine to presenting the model for the blood flow in the fibre channel, the plasma flow through the membrane, and the dialyzate counterflow, already reduced at the zero order approximation. We use the same symbols as in the ultrafiltration model. The typical fibre length is 20 cm, with radius 100 μm, implying $\varepsilon = 10^{-4} \div 10^{-3}$.

$$
\begin{cases}
(1+\zeta)\dfrac{\partial v_x^{(0)}}{\partial r} = \dfrac{r}{2}\dfrac{\partial P_h^{(0)}}{\partial x}, \quad \text{(blood flow)}, \\[2ex]
[1+\zeta]_{r=1}\, v_x^{(0)}\Big|_{r=1} = -\dfrac{1}{2\mathsf{B}_h}\dfrac{\partial P_h^{(0)}}{\partial x}, \quad \text{(slip at the interface)}, \\[2ex]
\displaystyle\int_0^1 r\frac{\partial v_x^{(0)}}{\partial x} dr = \frac{S\mathsf{G}}{\ln H}\left(P_s^{(0)} - P_h^{(0)}\right), \quad \text{(cross flow)}, \\[2ex]
P_h^{(0)}\Big|_{x=0} = 1, \quad P_h^{(0)}\Big|_{x=1} = 0, \quad \text{(blood inlet/outlet pressure)}, \\[2ex]
\dfrac{\partial^2 P_s^{(0)}}{\partial x^2} = A_1\left(P_s^{(0)} - P_h^{(0)}\right), \quad \text{(dialyzate flow)}, \\[2ex]
P_s^{(0)}\Big|_{x=0} = -\mathfrak{P}_2, \ P_s^{(0)}\Big|_{x=1} = -\mathfrak{P}_1 - \mathfrak{P}_2, \ \text{(dialyzate inlet/outlet pressure)}, \\[2ex]
\dfrac{\partial \varphi^{(0)}}{\partial t} + \left(2\displaystyle\int_0^1 r\, v_x^{(0)} dr\right)\dfrac{\partial \varphi^{(0)}}{\partial x} = 2\varphi^{(0)}\dfrac{S\mathsf{G}}{\ln H}\left(P_h^{(0)} - P_s^{(0)}\right), \quad \text{(hematocrit evolution)}, \\[2ex]
\varphi|_{x=0} = \dfrac{1}{1 + V_o - 2\mathfrak{V}\dfrac{S\mathsf{G}}{\ln H}\displaystyle\int_0^t\int_0^1\left(P_h^{(0)} - P_s^{(0)}\right) dx\, d\tau}, \quad \text{(inlet hematocrit)}, \\[2ex]
\varphi(x,0) = \varphi_o, \quad \text{(initial hematocrit)}.
\end{cases}
$$

Here ζ is generally a function of the hematocrit φ and of the shear rate (blood rheology is characterized by shear thinning), G is a dimensionless constant proportional to the membrane permeability, A_1 contains geometrical elements and is proportional to G. The coefficient B_h in the second equation decides the level of slip at the fibre wall (a value $\sim$ 2.5 can be identified from experimental observations). The coefficient $\mathfrak{V}$ is the ratio between the blood capacity of the device and the total RBC's volume in the patient's blood. The coefficient $\mathfrak{P}_1$ is the ratio between the pressure difference driving the dialyzate flow and the one driving the blood flow, the coefficient $\mathfrak{P}_2$ is the ratio (outlet blood pressure - inlet dialyzate pressure)/(blood pressure drop). A peculiar aspect is represented by the inlet hematocrit condition, which keeps track of the history of the treatment and is also depending on $P_h^{(0)} - P_s^{(0)}$, in a nonlocal way. The latter difference can be shown to be always positive. The analysis of the system above is quite complicated, but if for instance one sets $\zeta = 0$ then the evolution of φ along the fibre can be calculated explicitly, so that it is possible to derive good estimates of the parameters ranges that guarantee the regular operation of the device.

Once the fluid dynamical problem has been solved the extraction from blood of chemicals like urea, etc. can be calculated. Here too a nonlocal inlet boundary condition comes into play. For all these details, as well for an existence and uniqueness theorem we refer to [6].

Acknowledgments

This work was partially supported by the European Commission by means of the project *PURIFAST* (Advanced Purification Of Industrial and Mixed Wastewater by Combined Membrane Filtration and Sonochemical Technologies), within the program *LIFE+ 2007* - Contract N. ENV/IT/00439 - January 2009 - December 2011.

References

[1] G.S. Beavers., D.D. Joseph, Boundary conditions at a naturally permeable wall, *J. Fluid Mech.*, **30** (1967) 197–207.

[2] I. Borsi, A. Fasano, Modelling waste water flow in hollow fibre filters. Proc. Comsole Conference, (2009).

[3] I. Borsi, A. Farina, A. Fasano, On the influence of geometrical factors and of slip condition on the filtration through hollow fibres, submitted to *ZAMP*

[4] G. Belfort, R.H. Davis, A.L. Zydney, The behavior of suspensions and macromolecular solutions in crossflow microfiltration, *J. Membrane Sci.*, **96** (1994) 1–58.

[5] W.J. Bruining, A general description of flows and pressures in hollow fiber membrane modules, *Chem. Eng. Sci.*, **44** (1989) 1441–1447.

[6] A. Farina, A. Fasano, Modelling high flux hollow fibres dialyzers. Submitted.

[7] A. Farina, A. Fasano, Designing irrigation pipes. Submitted.

[8] S. Eloot, D. De Wachter, I. Van Trich, P. Verdonck, Computational flow in hollow–fiber dialyzers, *Artificial Organs*, **26** (2002) 590–599.

[9] J. Himmelfarb, T.A. Ikizler, Hemodialysis, *N. Engl. J. Med.*, **363** (2010) 1833-1845.

[10] W. Jäger, A. Mikelić, Modeling effective interface laws for transport phenomena between an unconfined fluid and a porous medium using homogenization, *Transp. Porous Med.*, **78** (2009) 489–508.

[11] M. Labecki, J.M. Piret, B.D. Bowen, Two-dimensional analysis of fluid flow in hollow–fiber modules, *Chem. Eng. Sci.*, **50** (1995) 3369–3384.

[12] N. P. Reddy, Design of Artificial Kidneys, in Biomedical Engineering and Design Handbook, Volume 2: Applications, (2nd Edition), M. Kutz Ed., Mc Graw Hill, New York, 2009.

[13] O.E. Robey, Porous hose irrigation, *Michigan Extension Bulletin*, **133** (1934), 1–22.

[14] P. Saffman, On the boundary condition at a surface of a porous medium, *Stud. Appl. Matgh.,* **50** (1971) 93–101.

[15] F.J. Valdés-Parada, J. Alvarez-Ramírez, B. Goyeau, J.A. Ochoa-Tapia, Computation of jump coefficients for momentum transfer between a porous medium and a fluid using a closed generalized transfer equation, *Transp. Porous Med.*, **78** (2009) 439–457.

[16] L.J. Kelsey, M.R. Pillarella, A.L. Zydney, Theoretical-analysis of convective flow profiles in a hollow-fiber membrane bioreactor, *Chem. Eng. Sci.* **45** (1990) 3211-3220.